Translational Research in Anatomy 37 (2024) 100352

Contents lists available at ScienceDirect

Translational Research in Anatomy

journal homepage: www.elsevier.com/locate/tria

Arbor vitae cerebelli: Fractal properties and their quantitative assessment by novel "contour scaling" fractal analysis method (an anatomical study)

Nataliia Maryenko *, Oleksandr Stepanenko

Department of Histology, Cytology and Embryology, Kharkiv National Medical University, Kharkiv, Ukraine

ARTICLE INFO

Keywords:
Anatomy
Brain
Cerebellum
Fractals
White matter

ABSTRACT

Background: Arbor vitae cerebelli (tree-like branching white matter of the cerebellum) has a complex spatial configuration that is challenging to assess using conventional morphometric methods. This study proposes a fractal approach to describe and quantify the anatomy of Arbor vitae cerebelli. For this purpose, a new "contour scaling" method for fractal analysis of cerebellar white matter was developed.

Material and methods: The cerebella of 100 cadavers (50 male and 50 female) who died from causes unrelated to brain pathology, aged 20–95 years, were examined. Mid-sagittal sections of the cerebellar vermis were studied. The fractal dimension values of the cerebellar white matter were determined using both the developed fractal analysis method and the conventional "box counting" method, along with measurements of non-fractal parameters including cerebellar weight, area and perimeter of the vermis cross-section, perimeter-to-area ratio, and circularity.

Results: Considering the cerebellar white matter as a tree-like fractal, it was found to have 7 or 8 primary branches, which subdivide into 10-18 second-iteration branches, 19–38 third-iteration branches, and 34–53 fourth-iteration branches. Females more often had 8 primary branches compared to males, while males had a greater number of branches in the second to fourth iterations. The mean fractal (Hausdorff) dimension was 1.697 (1.721 in males, 1.674 in females, $P = 0.01$). The fractal dimension correlated most strongly with the perimeter and area of the vermis cross-section and had no significant relationship with age.

Conclusion: The fractal (Hausdorff) dimension, determined using the novel "contour scaling" method, quantitatively assesses the degree of branching of the cerebellar white matter. An increase in the absolute size of the cerebellum leads to a higher degree of branching of its white matter and an increase in the number of its constitutive components – white matter branches and folia.

1. Introduction

The cerebellum, with its intricate architecture of white matter and cortex, poses a significant challenge for morphological analysis. The primary contributor to the complexity of the cerebellum's spatial configuration is the folding of its surface, which is manifested in the elaborate patterns of foliation and fissuration – divisions of cerebellar tissue into lobes, lobules, and the separation of individual cortical gyri, known as folia [1]. This structural complexity results in a high degree of anatomical variability in the cerebellum, both interspecies and intraspecies [2]. Notably, the characteristics of cerebellar foliation and fissuration vary, generally becoming more complex along the phylogenetic sequence of different species [3] and throughout prenatal cerebellar development [4,5]. Additionally, abnormalities in cerebellar foliation and fissuration are observed in cases of cerebellar malformations [6–8].

However, foliation and fissuration, which characterize the surface configuration of the cerebellum, are not the only features reflecting its anatomical complexity. While most researchers have focused on these surface characteristics [1,3–8], we chose to delve deeper, examining the complexity of the Arbor vitae cerebelli – the tree-like branching white matter of the cerebellum that forms the basis ("scaffold") of its cortex. The greater the branching of the white matter, the more pronounced the foliation and fissuration of the cerebellar cortex. It can be hypothesized that variations in foliation and fissuration in phylogenetic and ontogenetic contexts, as well as in malformations, are rooted in differences in the degree of white matter branching. Additionally, that differences in

* Corresponding author. Department of Histology, Cytology and Embryology, Kharkiv National Medical University, Kharkiv, 4 Nauky avenue, 61022, Ukraine.
E-mail addresses: maryenko.n@gmail.com, ni.marienko@knmu.edu.ua (N. Maryenko), stepanenko.kharkiv@gmail.com, oy.stepanenko@knmu.edu.ua (O. Stepanenko).

https://doi.org/10.1016/j.tria.2024.100352
Received 5 August 2024; Received in revised form 6 September 2024; Accepted 9 September 2024
Available online 10 September 2024

cerebellar structural complexity could serve as anatomical criteria for diagnosing cerebellar malformations (and distinguishing them from acquired cerebellar atrophy), as well as for fundamental anatomical, anthropological, or biological research. However, a critical question is raised: how can a structure with such complex and variable architecture be quantitatively and objectively characterized?

Among the morphometric methods for studying the cerebellum, those derived from Euclidean ("classical") geometry are most commonly used – measuring the linear dimensions of the cerebellum [9,10], cross-sectional area [10,11], and the volume of the cerebellum as a whole or its individual parts [12,13]. However, the spatial complexity of the cerebellum's configuration is difficult to assess using these morphometric methods. To characterize the degree of cerebellar shape complexity, various researchers have attempted to develop alternative quantitative or semi-quantitative assessment methods. For instance, in studies of chondrichthyan cerebella, the shape complexity (degree of foliation) was visually assessed by three independent experts who assigned scores from 1 to 5 [14,15]. To characterize foliation in avian cerebella, a gyrification index was calculated [16,17]. A descriptive approach was used to characterize the anatomy and branching of human cerebellar white matter [18].

In this study, a fractal approach was applied to the anatomy of the Arbor vitae cerebelli, viewing the cerebellar white matter as a tree-like fractal to enable the determination of its fractal dimension, which characterizes the complexity of fractal structures [19,20]. To achieve this, a simple and applicable fractal analysis method, termed the "contour scaling" method, was developed. Additionally, the study aimed to characterize the variability in human cerebellar white matter branching complexity using the developed fractal analysis method and to identify factors influencing the complexity of the Arbor vitae cerebelli.

2. Fractal principle of cerebellar anatomy

A fractal is a self-similar or self-affine figure, whose parts replicate (exactly or approximately) the structure of the whole [19–21]. This key property of fractals is referred to as self-similarity or self-affinity. A fractal is self-similar if its structure looks the same at different scales. A fractal is self-affine when its structure appears similar at different scales, but the scaling factors differ along different dimensions. Self-similarity and self-affinity give fractals scale invariance, meaning that their structure remains consistent across different scales [19–21]. Self-similarity involves uniform scaling in all directions (isotropic scaling), while self-affinity involves non-uniform scaling across different directions (anisotropic scaling). Self-similar fractals tend to have exact, repeating patterns, while self-affine fractals may exhibit more irregular patterns, where repetition is scale-dependent and varies by direction.

The complexity of a fractal's structure is quantified by its Hausdorff dimension, a specific type of fractal dimension [19–22]. Fractals include artificial (mathematical) fractals, which have a mathematically defined algorithm for their development and therefore a known Hausdorff dimension, as well as natural fractals (quasi-fractals), which exhibit fractal properties but lack a strict mathematical algorithm, and thus do not have a known Hausdorff dimension [22]. Natural fractals more comonly exhibit self-affinity rather than self-similarity, resulting in a more irregular structure.

A clear example of fractals is fractal trees, with the classic example being the Pythagoras (Pythagorean) tree (Fig. 1) [23,24], whose Hausdorff dimension equals 2 [23]. The construction (development) of artificial fractal trees involves multiple stages – iterations (repeated, similar actions) [19–24]. During each iteration, the Pythagoras tree undergoes a dichotomous division: two branches in the form of squares are added, with their combined area equaling the area of the squares from the previous iteration. The side length of the "child" squares is given by $L_1 = L_0/\sqrt{2}$, where L_0 is the side length of the "parent" square, and L_1 is the side length of the "child" square in the first iteration. The scaling factor M is computed as $M = (L_{i-1})/L_i$. For the Pythagoras tree, the scaling factor is $\sqrt{2}$. The Hausdorff dimension of mathematical fractals is determined using formula $D = \ln(N)/\ln(M)$, where D represents the Hausdorff dimension, N is the number of constituent parts of the fractal (the number of "child" branches that emerge from a "parent" branch at each iteration), and M is the scaling factor. Consequently, the Hausdorff dimension of the Pythagoras tree is $D = \ln(2)/\ln(\sqrt{2}) = 2$.

The Arbor vitae cerebelli can be regarded as a natural fractal tree, given that its anatomy conforms to fractal principles. From the corpus medullare cerebelli, seven or eight primary branches of white matter extend directly, forming the basis of the ten classical cerebellar lobules [25]. In some instances, Lobule III (Lobulus Centralis II) may be absent, exemplifying individual anatomical variability [2,18,25]; in such cerebella, the corresponding third branch of white matter is absent, resulting in seven branches instead of eight extending from the corpus medullare [25]. It is proposed to consider these initial seven or eight branches of white matter as the first iteration of the fractal organization of the Arbor vitae (Fig. 2). This is followed by two to three iterative divisions of the branches, which split into two or three sub-branches. The final iteration consists of small surface branches (folia with a white matter core), forming the visible surface of the cerebellum. The branches of different iterations tend to exhibit similar branching patterns, typically a dichotomous Y-shaped branching, or, in rare cases, a division of the main trunk into three branches. However, the white matter branching patterns show a high degree of individual anatomical variability and do not replicate exactly across different scales. The branching patterns of 1st, 2nd, or 3rd iteration branches may not coincide. Therefore, the Arbor vitae branching pattern is more appropriately described as self-affine rather than self-similar. Since the cerebellum does not have a clear mathematical construction algorithm, and exhibits self-affinity rather than self-similarity, determining its Hausdorff dimension as for the Pythagoras tree is very challenging. Therefore, it was aimed to develop an alternative counting method.

3. Material and methods

3.1. Material

The study utilized cadaveric material, specifically cerebella from individuals who had died of causes unrelated to neurological pathology and exhibited no pathological changes in the brain. The sample

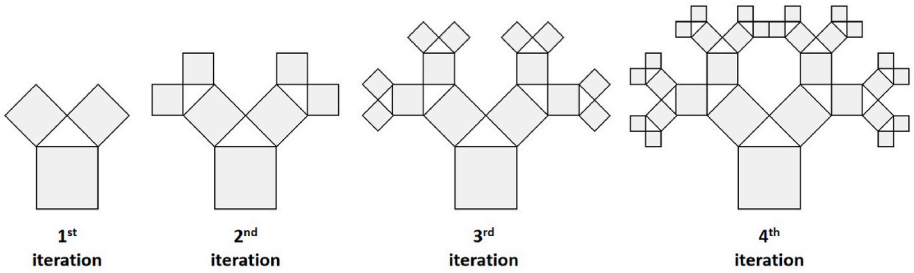

Fig. 1. Stages of development of the tree-like mathematical fractal – Pythagoras Tree.

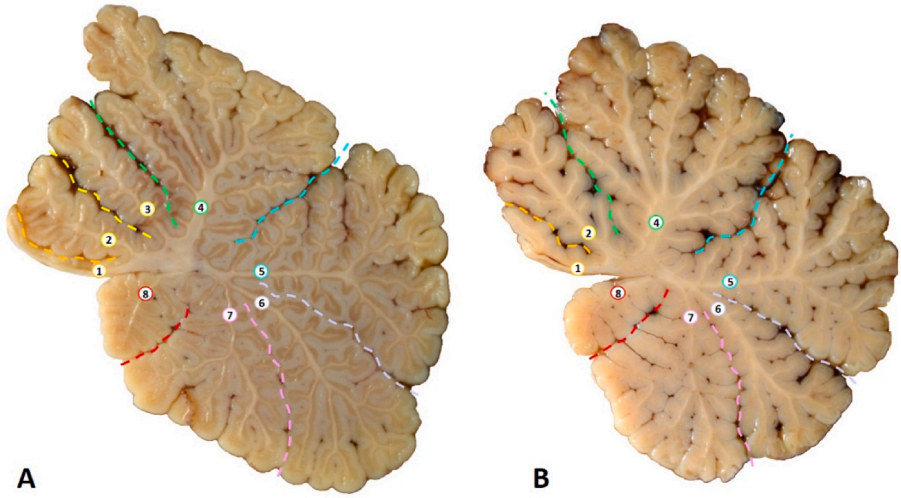

Fig. 2. Arbor vitae cerebelli: mid-sagittal section of the cerebellar vermis; the primary white matter branches of the first iteration are indicated by Arabic numerals. A – cerebellum with 8 primary branches, B – cerebellum with 7 primary branches (the third branch is absent).

comprised cerebella from 100 cadavers obtained during forensic autopsies, including 50 male and 50 female subjects. The age range of the sample was 20–95 years (males: 20–88 years; females: 22–95 years). The distribution by age groups was as follows: 20–30 years – 10 subjects (8 males, 2 females); 31–45 years – 14 subjects (11 males, 3 females); 46–60 years – 31 subjects (15 males, 16 females); 61–75 years – 18 subjects (11 males, 7 females); 76–95 years – 27 subjects (5 males, 22 females).

3.2. *Preparation of anatomical specimens, non-fractal morphometry*

After the cerebellum was separated from the brainstem, its weight was determined. Subsequently, the cerebellum was fixed for one month in 10 % neutral buffered formalin. Following fixation, the cerebellum was sectioned in the mid-sagittal plane using a microtome blade, and parallel parasagittal sections were made in the para-vermal region at a distance of 5 mm to the right and left of the mid-sagittal section using a slicer. The mid-sagittal section of the cerebellar vermis was then photographed with a morphometric ruler placed alongside (Fig. 3).

The macro-photographs were analyzed to determine the cross-sectional area (A) and perimeter (P) of the vermis. From these measurements, the perimeter-to-area ratio (P/A) was calculated, along with the shape factor (SF), or circularity. The shape factor was computed using the formula: $SF = (4\pi \times A)/P^2$ [26].

Fig. 3. Macro-photograph of the mid-sagittal section of human cerebellar vermis. The labeled division of the morphometric ruler is 1 cm, the smallest (unlabeled) division is 1 mm.

3.3. *Fractal analysis of arbor vitae cerebelli: conventional "box counting" method*

First, a fractal analysis of the Arbor vitae cerebelli was conducted using the conventional "box counting" method [27], which is widely used in medicine and morphology. This method calculates the Minkowski dimension (also known as the box-counting dimension), a specific type of fractal dimension. For the study, image fragments with an absolute size of 4 × 4 cm (1024 × 1024 pixels), containing cross-sections of the cerebellar vermis, were utilized (Fig. 4A).

In the first stage of the study, the fractal properties of white matter at various possible scales were examined. To do this, regions corresponding to the white matter of the cerebellum were manually outlined and colored black on a macro-photograph of an unstained section of the cerebellar vermis (Fig. 4B). As a result, a binary (black-and-white) mask of the white matter was obtained (Fig. 4C). Automated fractal analysis of the binary image in Fig. 4C was performed using the "fractal box count" tool of the ImageJ software [28].

The principle of the classical "box counting" method is as follows. The image is iteratively divided into boxes of a specified size (Box size), and the number of "filled" boxes intercepting (containing) fragments of the structure under study (N) is counted (Fig. 4D–H). Fractal analysis involves several stages, the number of which can vary. In the case of Arbor vitae cerebelli, 18 stages of fractal analysis were used with the following Box sizes: 1, 2, 3, 4, 6, 8, 12, 16, 24, 32, 48, 64, 96, 128, 192, 256, 384, 512 pixels (Table 1).

To determine the fractal dimension (Minkowski dimension), the natural logarithms of N and 1/Box size are calculated, after which the linear regression equation $y=bx+a$ is computed, where ln(1/Box size) is the independent variable (x) and ln(N) is the dependent variable (y). The fractal dimension corresponds to the slope (coefficient b) of the regression line, and coefficient a is an estimated intercept (Fig. 5). As shown in Fig. 5, the Minkowski dimension after 18 stages of fractal analysis was 1.593.

The plot of ln(N) versus ln(1/Box size) (Fig. 5) exhibits a linear pattern with a single slope segment, indicating the monofractal behavior of the Arbor vitae cerebelli across a wide range of scales. This also suggests that the Arbor vitae cerebelli can be classified as a thin ("ordinary") fractal, as its fractal dimension has fractional, rather than integer values, characteristic of fat fractals.

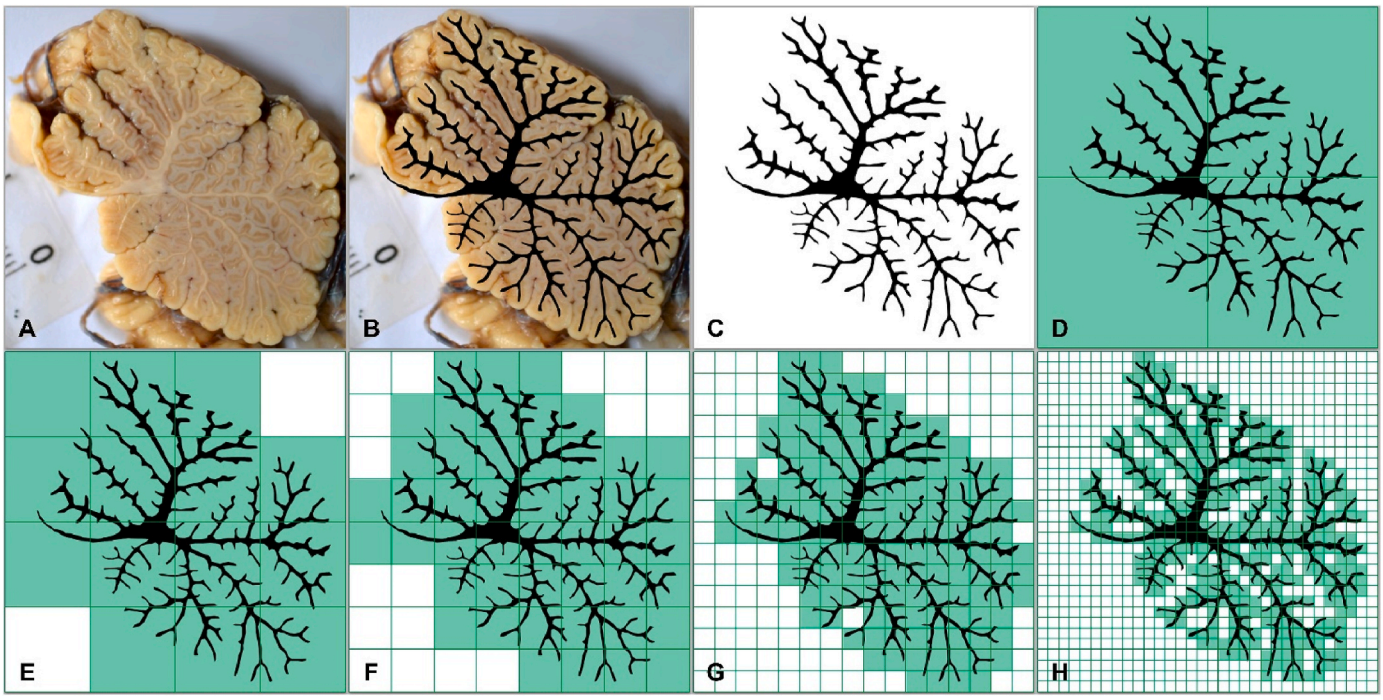

Fig. 4. The principle of the conventional "box counting" method used for the fractal analysis of the Arbor vitae cerebelli. A – initial (unstained) image; B – highlighting the Arbor vitae cerebelli in the image; C – binary mask of the Arbor vitae cerebelli; D-H – fractal analysis with fractal grids of different Box sizes: D – Box size of 1/2; E – Box size of 1/4; F – Box size of 1/8; G – Box size of 1/16; H – Box size of 1/32; the "filled" boxes, intercepting (containing) the studied structure, are highlighted with a darker background.

Table 1
Data for determining the fractal dimension of arbor vitae cerebelli using "box counting" method.

Stage of fractal analysis (iteration)	N	ln(N)	Box size (pixels)	Box size (fractional)	1/Box size	ln(1/Box size)
1	125043	11.736	1	1/1024	1024	6.931
2	34585	10.451	2	1/512	512	6.238
3	16830	9.731	3	3/1024	341.33	5.833
4	10252	9.235	4	1/256	256	5.545
5	5274	8.571	6	3/512	170.67	5.140
6	3379	8.125	8	1/128	128	4.852
7	1834	7.514	12	3/256	85.33	4.447
8	1254	7.134	16	1/64	64	4.159
9	710	6.565	24	3/128	42.67	3.753
10	479	6.172	32	1/32	32	3.466
11	259	5.557	48	3/64	21.33	3.060
12	159	5.069	64	1/16	16	2.773
13	76	4.331	96	3/32	10.67	2.367
14	48	3.871	128	1/8	8	2.079
15	24	3.178	192	3/16	5.33	1.674
16	14	2.639	256	1/4	4	1.386
17	9	2.197	384	3/8	2.67	0.981
18	4	1.386	512	1/2	2	0.693

Similarly, binary images of the Pythagoras tree at the 3rd, 4th, and 5th iterations (image size 1024 × 1024 pixels, Box sizes: 1, 2, 3, 4, 6, 8, 12, 16, 24, 32, 48, 64, 96, 128, 192, 256, 384, 512 pixels) were tested and demonstrated similar monofractal behavior across different scales (Fig. 6). However, the obtained Minkowski dimension values (1.75, 1.72, and 1.74) did not match the Hausdorff dimension of 2. This discrepancy indicates that these dimensions characterize different aspects of the spatial organization of fractals.

For further fractal analysis of the Arbor vitae cerebelli using the "box counting" method, 30 younger individuals (aged 20–47 years) were selected from the main sample of 100, to minimize the impact of age-related changes on fractal dimension values. Since unstained specimens were used, segmentation (as in Fig. 4A–C) could only be performed manually. Therefore, it was decided to conduct the fractal analysis by manual counting the filled boxes without prior image segmentation. For manual counting, Adobe Photoshop CS5 software was used, applying a grid with boxes of a specified size to the image. The filled boxes were manually counted using the "Count Tool" (Fig. 7B). Four stages of fractal analysis were conducted with the following Box sizes: 1/4 (1 × 1 cm), 1/8 (0.5 × 0.5 cm), 1/16 (0.25 × 0.25 cm), and 1/32 (0.125 × 0.125 cm) (Fig. 4E–H). Given the linear nature of the ln(N) vs ln(1/Box size) plot across a wide range of scales (Fig. 5) and the resolution limitations of the image, it was decided to limit manual counting to the smallest Box size of 0.125 × 0.125 cm (Fig. 7).

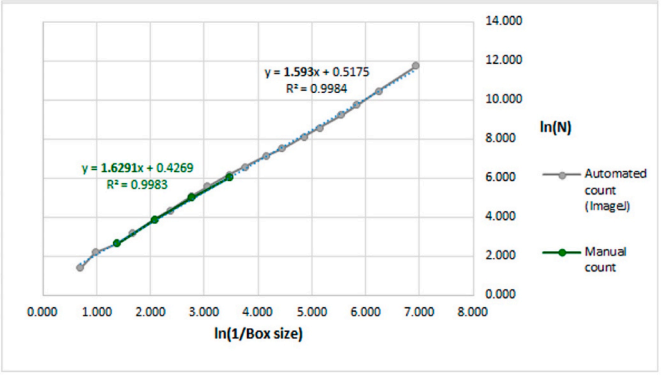

Fig. 5. Determining the fractal dimension (Minkowski dimension) of Arbor vitae cerebelli using the "box counting" method: the fractal dimension determined by automated counting is 1.593, and by manual counting is 1.6291.

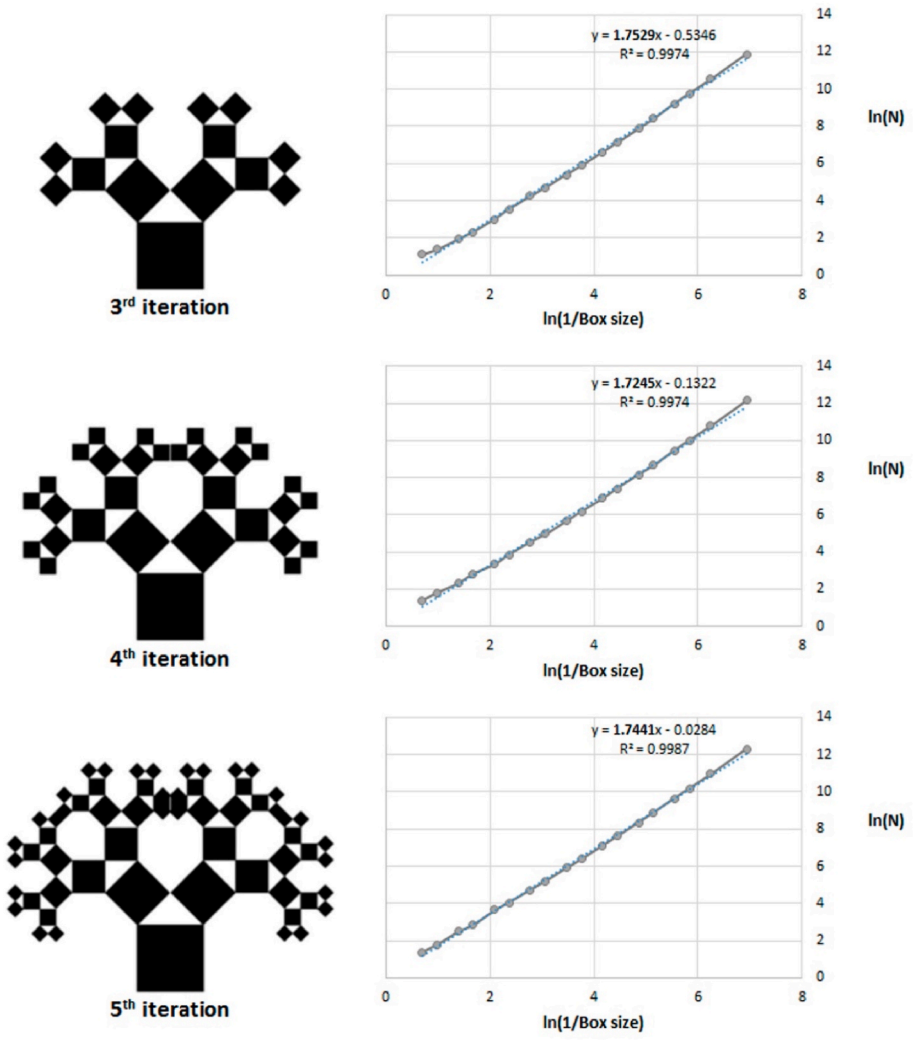

Fig. 6. The determining the fractal dimension (Minkowski dimension) of Pythagoras tree using "box counting" method (automated counting using ImageJ software).

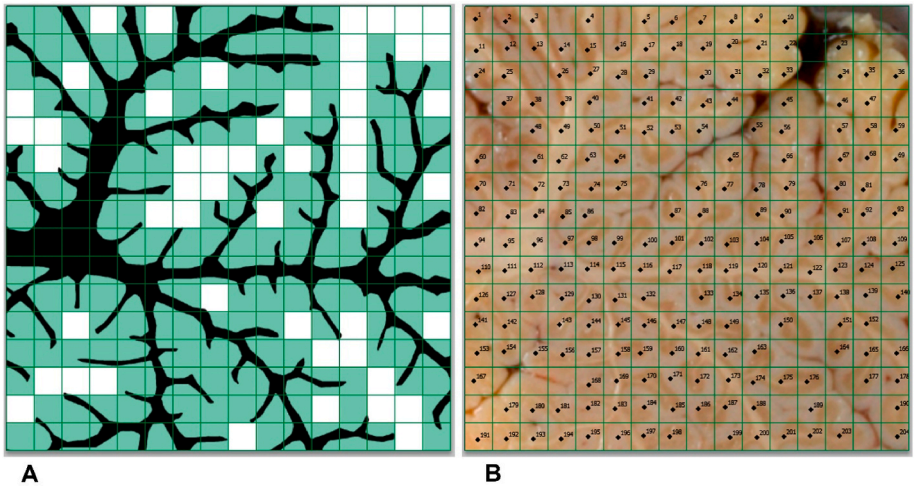

Fig. 7. Counting filled boxes using the "box counting" method for fractal analysis of the Arbor vitae cerebelli: A – principle of counting; B – manual counting using a non-segmented, unstained image with the "Count Tool" in Adobe Photoshop; a 1 × 1 cm fragment of the image is shown, with a Box size of 0.125 × 0.125 cm.

3.4. Fractal analysis of arbor vitae cerebelli: A novel "contour scaling" fractal analysis method

The developed approach is based on the classical "cumulative intersection" fractal analysis method, which is typically used for the fractal analysis of neurons [27]. In this method, circles of varying diameters are overlaid on an image, and the number of branches intersecting each circle is counted. The fractal dimension is then calculated based on the number of branches and the radii of the circles. This method was applied to the cerebellum (Fig. 8). However, using circles did not fully meet the requirements due to variations in the shape of the cerebellum and its midsagittal cross-section among individuals. As a result, branches were intersected differently, causing variations in how circles of the same diameter intersected branches at different iterations across different cerebella.

Since the configuration of the cerebellum varies, we propose using the contour of the cerebellum's external surface rather than circles (Fig. 9). The contours of the cerebellar cross-section, corresponding to the visible surface formed by the branches of the final iteration (similar to how the "crown" of artificial fractal trees is formed), were traced. The shape of the cerebellum and its lobules may vary, so using the cross-sectional contour allows for the replication of the cerebellum's anatomical shape. Given the monofractal nature of the Arbor vitae cerebelli, it can be assumed that the degree of space-filling by branches in different areas of the cerebellum does not differ significantly. Scaling the contours that follow the overall shape of the cerebellum in its cross-section enables the intersection of branches from equivalent iterations.

To align the contours with the anatomical features of the cerebellum, a "control point" corresponding to the vertex of the angle between velum medullare superior and inferior was used. After scaling, the control points of the four contours were aligned and positioned in the corresponding anatomical area of the cerebellum. This approach ensures that all scaled contours will intersect branches from same iterations.

To trace the contour, the "Freeform shape" ("Curve") tool in Microsoft PowerPoint was utilized. The generated contour was then copied and scaled according to a predetermined scale. To develop a methodology, the contour was scaled with a step of 5 % (5 %, 10 %, 15 %, and continuing in subsequent increments). The number of the branches that are intersected by contours (N) was calculated. The counting of branches was done manually.

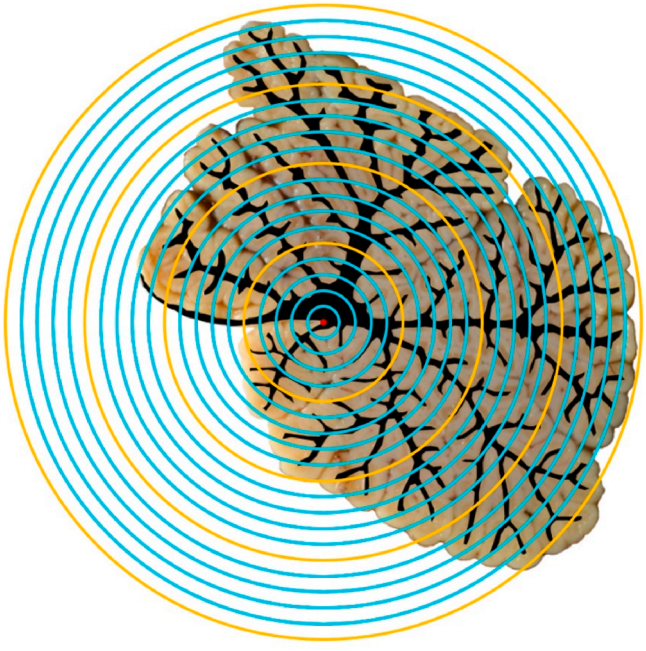

Fig. 8. Principle of the classical "cumulative intersection" fractal analysis method illustrated with the white matter of the cerebellum. The circles are scaled with a step of 5 % (compared to a biggest circle); the circles corresponding to a scales of 100 %, 75 %, 50 %, and 25 % are highlighted in orange. (For interpretation of the references to color in this figure legend, the reader is referred to the Web version of this article.)

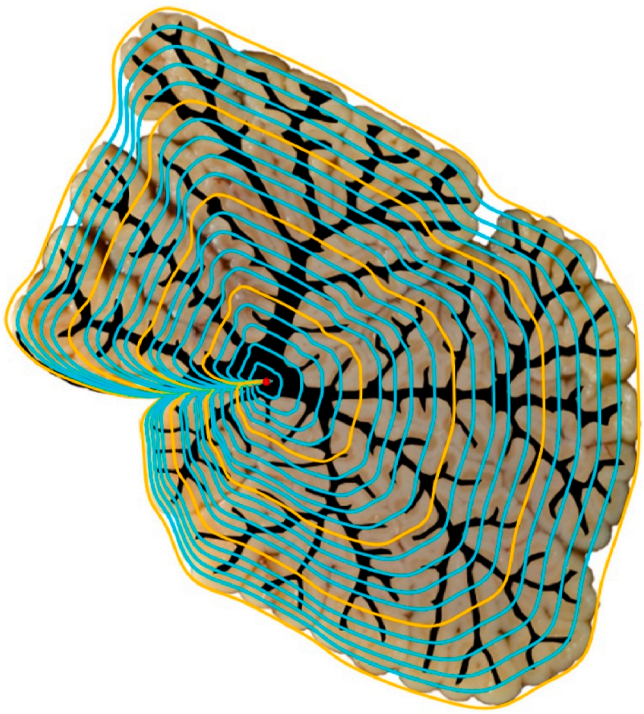

Fig. 9. Principle of the novel "contour scaling" fractal analysis method. The traced contours are overlaid on the midsagittal section of the cerebellar vermis and aligned using the control point (red) corresponding to the vertex of the angle between the velum medullare superior and inferior; contours are scaled with a step of 5 % (compared to a biggest, initial contour); the contours corresponding to a scales of 100 %, 75 %, 50 %, and 25 % are highlighted in orange. (For interpretation of the references to color in this figure legend, the reader is referred to the Web version of this article.)

To validate the developed fractal analysis method, the Pythagoras tree of 3rd, 4th, and 5th iterations was studied (Fig. 10). Its "crown" was traced by a smooth contour intersecting all squares (branches) of final iteration. The scaled contours were aligned with the center of the upper side of the "parent" square (the "trunk") which was used as a control point. The contours were also scaled with a step of 5 %, and number of intersected branches (N) was calculated.

To calculate the fractal dimension, it is necessary not only to determine the number of branches N but also to establish the scaling factor M. The original "cumulative intersection" method uses the radius or diameter of circles overlaid on the image as the scaling factor. Since scaled contours were utilized rather than circles, the fractal measure can be based on the relative scale of the contours, which changes proportionally to the radius of the circles used in the original "cumulative intersection" method. Therefore, the scaling factor Msc, determined based on the relative scale in the first stage of fractal analysis, was 0.05 (the smallest contour, representing 5 % of the original), for the second stage, Msc was 0.10 (10 %), for the third stage – 0.15 (15 %) and so on. In the final stage, it was 1 (100 %).

Next, the natural logarithms of the two numbers N and Msc were calculated. Based on these data, plots showing the relationship between ln(N) and ln(Msc) were constructed (Figs. 10 and 11). As seen from the graphs, this relationship is non-linear and fundamentally different from that observed when using the "box counting" method for fractal analysis

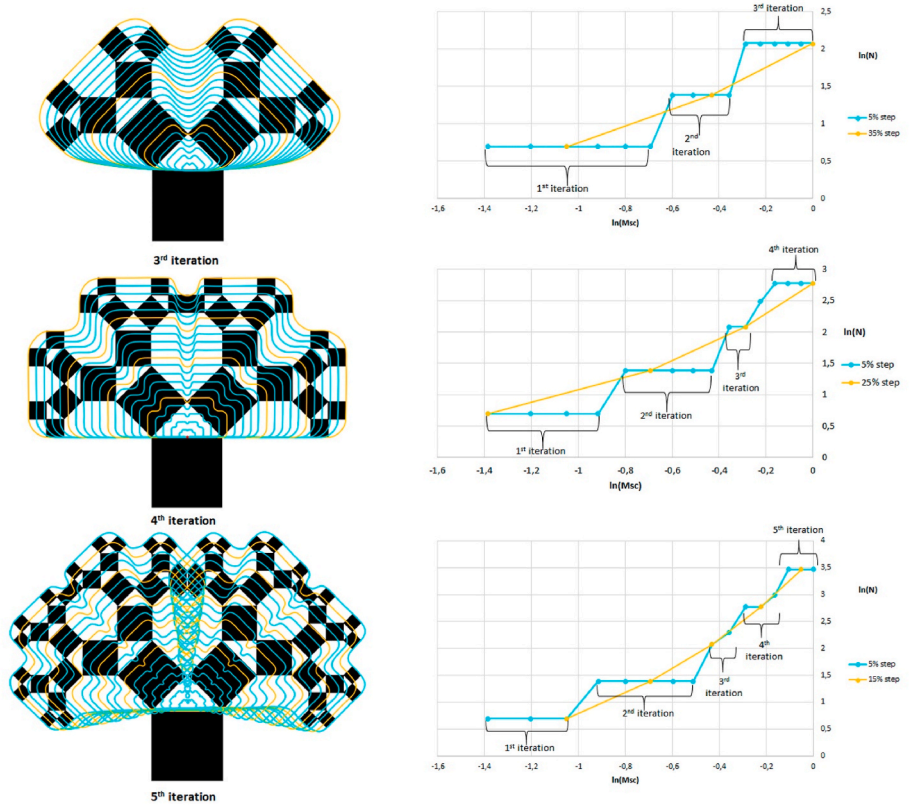

Fig. 10. Fractal analysis of Pythagoras tree using novel "contour scaling" method; contours are scaled with a step of 5 % (compared to a biggest, initial contour).

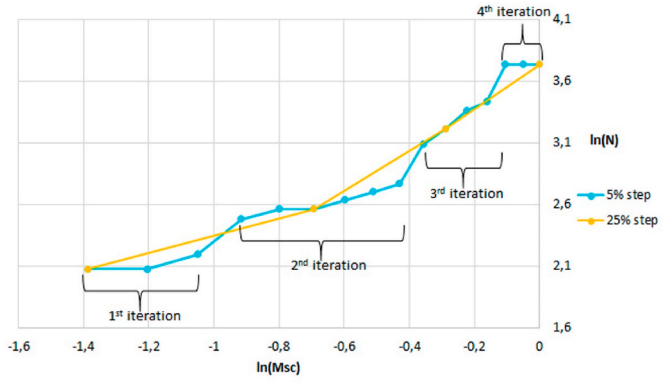

Fig. 11. Fractal analysis of Arbor vitae cerebelli using novel "contour scaling" method.

(Figs. 5 and 6). However, this pattern is expected given the characteristics of the new method: the scaled contours, which follow the "crown" shape of the tree-like fractal, intersect branches of the same or adjacent iterations. For example, several contours scaled in 5 % increments consistently intersect two branches of the first iteration of the Pythagoras tree, then several following contours intersect four branches of the second iteration, and so on. This results in "steps" on the graph corresponding to the respective iterations. In the ln(N) vs ln(Msc) plot for the Pythagoras tree analysis, three, four, or five distinct "steps" can be observed, corresponding to the three, four, or five iterations in the formation of these fractal trees (Fig. 10). Thus, small-step analysis does not merely verify mono- or multifractality but also identifies the number of iterations involved in forming the fractal tree and determines the scale ranges corresponding to branches of specific iterations.

In the ln(N) vs ln(Msc) plot for the Arbor vitae of the cerebellum (Fig. 11), four "steps" corresponding to four iterations are observed confirming the presence of the branches of four iterations. The presence of well-defined "steps" confirms that the scaled contours corresponding to the outer surface of the cerebellum consistently intersect branches from the same iterations.

To calculate the fractal dimension using the "contour scaling" method, it is advisable to use the number of fractal analysis stages (iterations) that correspond to the number of iterations in the studied fractal. The scales for the contours should be chosen so that they clearly intersect the branches of defined iteration. For the cerebellum, as a monofractal structure with four iterations, scales of 25 %, 50 %, 75 %, and 100 % were selected. For the Pythagoras tree with 3 iterations, the appropriate scales were 100 %, 65 %, and 30 % (a 35 % step); for 4 iterations, scales of 25 %, 50 %, 75 %, and 100 % (a 25 % step); and for 5 iterations, scales of 35 %, 50 %, 65 %, 80 %, and 95 % (a 15 % step). For monofractal structures, the intervals between contour scales are expected to be equal or proportional, while for multifractals, disproportionate intervals between scales may correspond to different iterations. Therefore, it is recommended to begin the analysis with small increments to determine the number of iterations and the scale ranges corresponding to each, then retain one contour (step) for each iteration.

The next task was to select the computational algorithm that would accurately determine the Hausdorff dimension. As a first attempt, the scaling factor Msc was employed (Table 2). The linear regression equation was calculated, where the independent variable is the natural logarithm of the scaling factor M, in this case, ln(Msc). The dependent variable is ln(N) (Fig. 12). The fractal dimension is determined as the estimated slope of the regression line. Therefore, the calculated fractal dimension of the 4th iteration Pythagoras tree was 1.459 ($r^2 = 0.96$).

However, the fractal dimension of the Pythagoras tree determined using the scaling factor Msc does not correspond to its true Hausdorff dimension (D = 2). Therefore, we decided to select an alternative scaling factor for the calculations. Since the Hausdorff dimension of mathematical fractals accounts for the change in branch length (side length of

Table 2
Data for determining the fractal dimension of Pythagoras tree.

Stage of fractal analysis (iteration)	N	ln(N)	Msc	ln (Msc)	L_i	Mbr = $1/L_i$	ln (Mbr)
1	2	0.693	0.25	−1.386	1	1	0
2	4	1.386	0.5	−0.693	$1/\sqrt{2}$	$\sqrt{2}$	0.347
3	8	2.079	0.75	−0.288	1/2	2	0.693
4	16	2.773	1	0	$1/2\sqrt{2}$	$2\sqrt{2}$	1.040

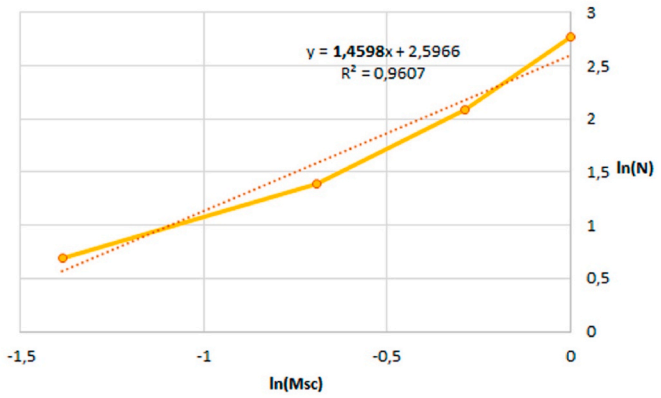

Fig. 12. Determining the fractal dimension of the Pythagoras tree based on the scaling factor Msc.

the square) at each iteration in the construction of a fractal tree, we opted to use this measure. Specifically, the length of each branch (side length of the square) L_i at each iteration decreases by a factor of $\sqrt{2}$ compared to the previous iteration. If the side length of the square at the first iteration is $L_1 = 1$, then at the second iteration it will be $L_2 = 1/\sqrt{2}$, at the third iteration $L_3 = 1/(\sqrt{2} \times \sqrt{2}) = 1/2$, and at the fourth iteration $L_4 = 1/(\sqrt{2} \times \sqrt{2} \times \sqrt{2}) = 1/2\sqrt{2}$ (Table 1). Thus, the scaling factor for the branches across different iterations is $Mbr_i = 1/L_i$.

By using ln(Mbr) instead of ln(Msc) as the independent variable, we recalculated the linear regression equation (Fig. 13). The resulting fractal dimension was 2 ($r^2 = 1$), which aligns with the true Hausdorff dimension of the Pythagoras tree. The testing of the developed algorithm on the 3rd and 5th iteration Pythagoras trees (Fig. 10) yielded the same fractal dimension value of 2.

To validate the obtained results, the developed algorithm was further tested on a binary tree with a scaling factor of $\sqrt{2}$ (Fig. 14); scales of 25

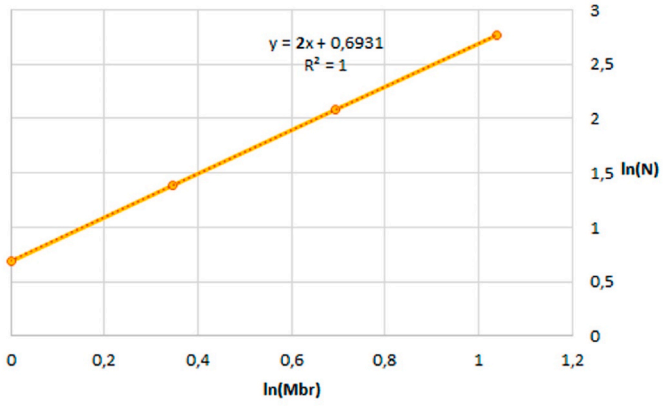

Fig. 13. Determining the fractal dimension of the Pythagoras tree based on the scaling factor Mbr.

%, 50 %, 75 %, and 100 % were selected. The Hausdorff dimension of the studied binary tree is $D = \ln(2)/\ln(\sqrt{2}) = 2$. The fractal dimension calculated using the novel method is also 2.

Therefore, the developed algorithm of fractal analysis was used to determine the fractal dimension of the Arbor vitae cerebelli. To demonstrate the fractal analysis algorithm, we used the cerebellum depicted in Fig. 9 as an example. This cerebellum had 8 primary branches of white matter extending directly from the corpus medullare and intersected by first contour. At the second stage, 13 s-order branches of 2nd iteration were intersected by second contour. At the third stage, 25 branches of 3rd iteration were identified, forming 42 terminal branches (surface folia) of 4th iteration intersected by the final contour (Table 3).

To calculate the fractal dimension based on the values in Table 3, the following analysis was performed; the Hausdorff dimension of the cerebellum depicted in Fig. 9 was found to be 1.6241 ($r^2 = 0.99$) (Fig. 15).

The algorithm for the described "contour scaling" fractal analysis method, is illustrated in Fig. 16.

3.5. Statistics

The statistical analysis was conducted using Microsoft Excel 2016. Descriptive statistics for the morphometric parameters are presented as the mean (M), standard error of the mean (SEM), standard deviation (SD), coefficient of variation (CV), median (Me), the 25th and 75th percentiles (Q1 and Q3, respectively), and minimum (min) and maximum (max) values. For discrete characteristics (number of branches), the count of objects (n) exhibiting specific characteristics was calculated. To determine differences between parameter values for males and females, and fractal dimensions determined by different fractal analysis methods, the Mann-Whitney *U* test was employed. Binary categorical attributes (presence of 7 or 8 primary white matter branches) in males and females were compared using the χ^2 test. To assess relationships between the obtained values, Spearman's rank correlation coefficient (R_S) was calculated, with significance evaluated using the Student's t-test. A statistical significance level of $\alpha = 0.05$ was chosen for the calculations.

4. Results

4.1. Calculation of cerebellar white matter branches

At the first stage of the analysis, the number of branches at each iteration forming the arbor vitae cerebelli was determined (Table 4).

In the studied sample, 7 primary branches of white matter extending from the corpus medullare were found in 62 % of cerebella (70 % in males and 54 % in females), while 8 primary branches were observed in 38 % (30 % in males and 46 % in females) (Table 4). The presence of eight primary branches was significantly more common in females compared to males ($P < 0.05$).

The number of second-iteration branches ranged from 10 to 18. The average number of these branches was significantly higher in males ($P = 0.047$). The number of third-iteration branches ranged from 19 to 28. Although the average number of third-iteration branches was also higher in males; however, this difference was not statistically significant ($P = 0.210$). The number of terminal branches in the fourth iteration ranged from 34 to 53 and was significantly higher in males compared to females ($P = 0.022$). Thus, the absolute number of branches at the 2nd to 4th iterations was greater in males, while females more frequently had a larger number of primary branches directly extending from the corpus medullare.

To determine how the relative number of branches changes across different iterations, the ratios of branches between successive iterations were calculated: the ratio of the number of second-iteration branches to the first, third-iteration branches to the second, and fourth-iteration branches to the third (Table 5).

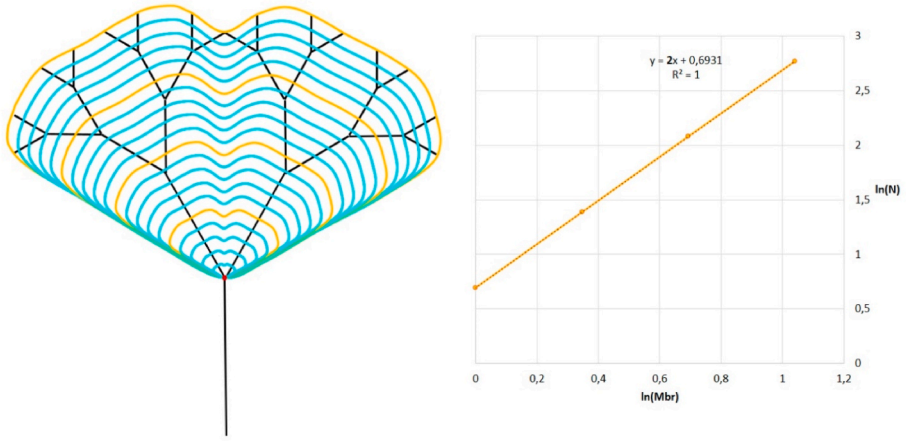

Fig. 14. Determining the fractal dimension of the binary tree (scaling factor $1/\sqrt{2}$) based on the scaling factor Mbr; contours are scaled with a step of 5 % (compared to a biggest, initial contour); the contours corresponding to a scales of 100 %, 75 %, 50 %, and 25 % are highlighted in orange, the corresponding steps were used in the analysis; the obtained fractal dimension equals 2. (For interpretation of the references to color in this figure legend, the reader is referred to the Web version of this article.)

Table 3
Data for determining the fractal dimension of cerebellar white matter.

Stage of fractal analysis (iteration)	N	ln(N)	Mbr = $1/L_i$	ln(Mbr)
1	8	2.079	1	0.000
2	13	2.565	$\sqrt{2}$	0.347
3	25	3.219	2	0.693
4	42	3.738	$2\sqrt{2}$	1.040

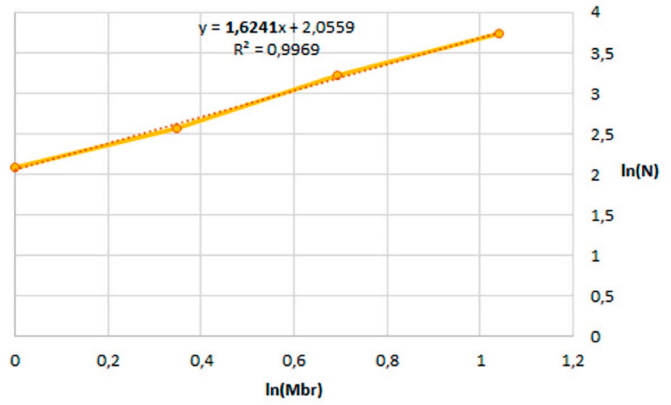

Fig. 15. Determining the fractal dimension (Hausdorff dimension) of the cerebellar white matter. The fractal dimension is 1.6241.

The ratios of the number of branches between different iterations were found to be quite similar. The highest ratio was observed between the number of second-iteration and first-iteration branches, while the lowest ratio was between the number of third-iteration and second-iteration branches. When comparing these ratios between males and females, it was found that the difference was statistically significant only for the ratio between the number of second-iteration and first-iteration branches ($P = 0.01$). The other two ratios did not show significant differences between males and females ($P > 0.05$).

4.2. Fractal dimension of the cerebellar white matter

The fractal dimension values of the cerebellar white matter calculated using two fractal analysis methods ("box counting" and "contour scaling") were significantly different ($P < 0.001$) (Table 6, Table 7). The determined fractal dimensions were significantly positively correlated, but the correlation relationship was moderate ($Rs = 0.495$).

The computed fractal dimension values varied within a narrow range, with the coefficient of variation not exceeding 6 %. However, a comparison between cerebella with relatively low and relatively high fractal dimension (Hausdorff dimension) values reveals that a cerebellum with a higher fractal dimension exhibits more extensive branching of the white matter (Fig. 17). When comparing fractal dimension values between males and females, it was found that males had significantly higher values ($P = 0.01$).

4.3. Non-fractal morphometric parameters of cerebellum and their relationships with fractal dimension

Descriptive statistics for additional (non-fractal) morphometric parameters of the cerebellum are provided in Table 8. The differences between all parameter values for males and females presented in Table 8 were statistically significant ($P < 0.001$ for all parameters).

The values of fractal dimensions determined by both fractal analysis methods were statistically significantly correlated with the absolute sizes of the cerebellum: its weight, area, and perimeter of the vermis cross-section (Table 9). The most significant correlation was observed with the perimeter and area. Thus, it can be concluded that an increase in the absolute size of the cerebellum leads to an increase in its fractal dimensions. Conversely, derived morphometric indices indicating the shape properties of the cerebellar vermis had a weak statistical relationship with fractal dimension values (Table 9). Notably, two fractal dimensions determined by different fractal analysis methods, demonstrated similar correlation relationships with non-fractal parameters.

4.4. Age-related changes of fractal dimension and non-fractal parameters of cerebellum

The values of fractal dimension did not show significant correlations with age in either males or females, whereas parameters characterizing the absolute sizes of the cerebellum statistically significantly decreased with age (Table 10).

5. Discussion

In this study, an analysis of the Arbor vitae cerebelli was performed using a fractal approach to characterize its anatomy. The cerebellum and its white matter can be considered fractal structures, exhibiting fractal principles of organization – self-affinity, self-replication at various scales, and numerous similar structural elements such as branches and

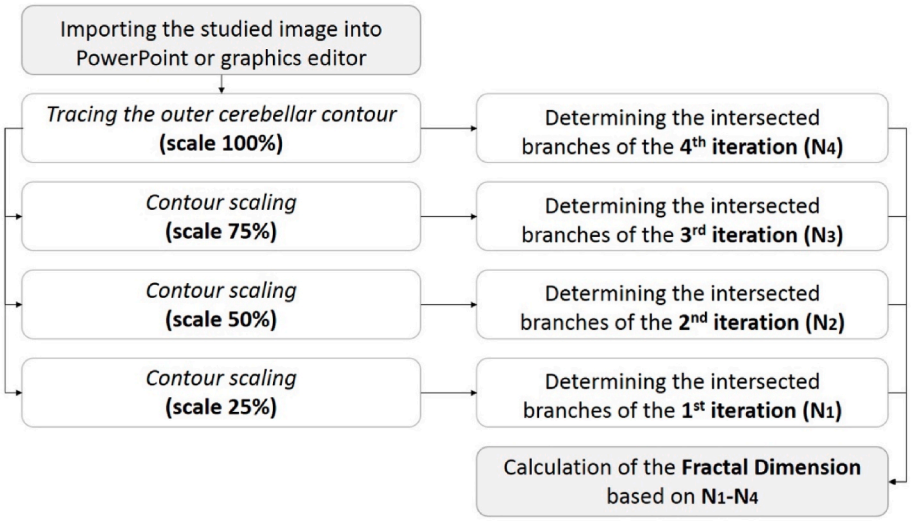

Fig. 16. Flow chart illustrating and summarizing novel "contour scaling" fractal analysis method.

folia. The analysis showed that the Arbor vitae cerebelli has approximately four iterations of branches, which may display similar, though not identical, branching patterns across different scales. The branching of cerebellar white matter appears somewhat irregular compared to artificial fractal trees. Therefore, the branching properties in the Arbor vitae cerebelli are better described as self-affinity rather than self-similarity.

The Arbor vitae cerebelli represents a natural fractal or quasi-fractal, differing from mathematical fractals in that it lacks a precise mathematical algorithm for its organization. The configuration of quasi-fractal structures may resemble that of artificial fractals or be more irregular, so different approaches may be applied for fractal analysis of such structures. Despite some irregularity, white matter of the cerebellum exhibits structure quite close to that observed in artificial fractal trees, enabling the determination of the Hausdorff dimension similar to how it is defined for artificial fractals.

The most closely related methods to the developed approach are the "cumulative intersection" method [29], the "convex hull" method [30], and the Sholl method [31], all of which are typically used for quantitative analysis of neuronal dendritic trees. Unlike existing fractal analysis methods – such as the "cumulative intersection" method and "convex hull" method – the developed method is specifically adapted for studying the cerebellum, taking into account its anatomical features and fractal organization patterns. In the classic "cumulative intersection" method, a series of circles are superimposed on the image, and the number of branches (of the neuronal dendritic tree) intersected by these circles is counted [29]. In contrast, the "convex hull" method, which is also used for neuronal analysis, involves outlining the dendritic tree with a smooth or broken contour that corresponds to the most peripheral dendritic termini (building a convex hull around them). This contour is then uniformly narrowed by a determined distance (number of pixels), and the number of branches intersecting the contour is counted [30]. Our method differs from these approaches in that it employs scaling rather than stepwise contour narrowing. Additionally, the contours are aligned using a control point to better match the anatomical structure of the cerebellum, whereas the "convex hull" method aligns contours around a common center. By outlining the overall cerebellar cross-section and fitting the scaled contours according to a control point, the current approach enables the counting of branches from the same iteration that are intersected by the same scaled contour. Consequently, the "contour scaling" method accommodates the anatomical variability of the cerebellum, which results in variations in the shape of its cross-section. Furthermore, the "contour scaling" method differs from both the "cumulative intersection" and "convex hull" methods in its calculation algorithm, which allows for the validation of results and the accurate determination of the true Hausdorff dimensions of mathematical fractal trees, as validated through the study of the Pythagoras tree and binary fractal tree.

The advantages of the proposed fractal analysis method include its simplicity and independence from scale. The "self-scaling" of the contour allows for more accurate calculations that are consistent with the cerebellum's structure and shape. Another benefit is that no specialized software is required – fractal analysis can be performed using PowerPoint or graphic editors capable of creating and scaling contours. Various types of images can be utilized, including anatomical macrophotographs, magnetic resonance images, or histological sections. Fractal analysis methods typically require adjustments based on image size, resolution, and other characteristics. For instance, in the "box counting" method, it is necessary to determine the range and values of the Box size (in pixels or other measures). The "convex hull" method involves narrowing the contour by a specified number of pixels. Commonly used automated "box counting" method (such as ImageJ or similar software) require image segmentation which is highly dependent on the image type and quality. The method presented in this study, however, only requires creating and scaling the cerebellar surface contour as a vector image when using PowerPoint software. The contour can be created and scaled using any image with sufficient clarity and visualization of the Arbor vitae cerebelli (or other branching structures). The studied image serves as a "background" while vector contours are scaled and overlaid on the image.

Several previous studies have also employed fractal analysis to investigate the cerebellum, primarily using magnetic resonance images [32–36]. However, all these studies utilized a different fractal analysis method – the "box counting" method – which is widely used in medical and morphological research due to its simplicity and versatility, and is thus rightly considered the "gold standard" of fractal analysis [27]. In our previous work, conducted with cadaveric specimens, we also used this method to study the cerebellar white matter [37]. What prompted the search for an alternative fractal analysis method? First and foremost, it was the routine and labor-intensive nature of the "box counting" method when applied to anatomical samples. Studying grayscale images (e.g., magnetic resonance images, computed tomography scans, angiograms, X-rays) with segmentation capabilities is simpler, as programs are available that can automate the counting of "filled" boxes after segmentation and binarization of images, such as the ImageJ software [28]. However, segmenting macrophotographs of anatomical samples (especially native, uncolored ones) is challenging, so the counting of "filled" boxes is done manually, increasing laboriousness and

Table 4
Distribution of the number of white matter branches in the cerebellum intersecting contours at different iterations during fractal analysis (n = 100).

1st iteration				2nd iteration				3rd iteration				4th iteration			
Number of branches	n (entire sample)	n (males)	n (females)	**Number of branches**	n (entire sample)	n (males)	n (females)	**Number of branches**	n (entire sample)	n (males)	n (females)	**Number of branches**	n (entire sample)	n (males)	n (females)
7	62	35	27	**10**	2	0	2	**19**	1	0	1	**34**	1	1	0
8	38	15	23	**11**	3	0	3	**20**	2	1	1	**35**	1	0	1
				12	15	7	8	**21**	4	3	1	**36**	2	1	1
				13	21	8	13	**22**	10	3	7	**37**	5	1	4
				14	28	17	11	**23**	19	8	11	**38**	5	2	3
				15	18	10	8	**24**	19	10	9	**39**	3	0	3
				16	7	6	1	**25**	27	14	13	**40**	5	3	2
				17	5	2	3	**26**	9	6	3	**41**	8	4	4
				18	1	0	1	**27**	5	2	3	**42**	11	5	6
								28	4	3	1	**43**	9	2	7
												44	12	6	6
												45	6	4	2
												46	4	2	2
												47	6	3	3
												48	10	9	1
												49	3	1	2
												50	4	3	1
												51	1	1	0
												52	2	1	1
												53	2	1	1
M	7.4	7.3	7.5	**M**	13.8	14.1	13.5	**M**	24.1	24.3	23.9	**M**	43.6	44.5	42.7

complicating the use of this method in anatomy.

Secondly, the nature of the methodologies differs: the "box counting" method determines a different type of fractal dimension, specifically the Minkowski dimension (box counting dimension) [19,20,24,37]. Although the Hausdorff and Minkowski dimensions are closely related and may coincide for some geometric figures, they describe different aspects of fractal geometry. The Minkowski dimension reflects the degree to which a structure fills space, as it involves partitioning space into boxes. In contrast, the Hausdorff dimension characterizes the complexity of the fractal based on the algorithm of its development. The "box counting" method is more versatile as it can analyze quasi-fractal structures with too irregular configuration (or even non-fractal structures). On the other hand, the Hausdorff dimension is generally determined for artificial fractals (or, as in this case, for structures with the configuration closely resembling artificial fractal trees). To clarify the relationship between the Minkowski and Hausdorff dimensions of the Arbor vitae cerebelli and to compare their values with those reported by other researchers, additional analysis was conducted on 30 cerebella (the younger group) using the conventional "box counting" method for fractal analysis. The fractal dimension values of cerebellar white matter determined by the "box counting" method (1.486 ± 0.013) were close to those reported in a study that employed the same method for two-dimensional magnetic resonance images (1.49 ± 0.06) [34]. However, the fractal dimensions determined in the present study by the "box counting" and "contour scaling" methods (Minkowski and Hausdorff dimensions) differed significantly. This difference can be explained as follows: Minkowski and Hausdorff dimensions typically coincide when analyzing simple geometric figures, such as lines, squares, or cubes, but in the case of fractal structures, these dimensions may not align. For instance, the present study showed that the "box counting" fractal analysis of the 3rd, 4th, and 5th iterations of the Pythagoras tree resulted in fractal dimensions that differed from its Hausdorff dimension. This finding is consistent with previous studies on artificial fractals [24,38]. The Minkowski dimension determined by the "box counting" method is influenced by characteristics such as branch and line thickness [38]. This can be an advantage when such characteristics are relevant to the study, but it can also be a disadvantage when it is necessary to mitigate the impact of these characteristics. Despite the differences in values, the two fractal dimensions were positively significantly correlated and exhibited similar relationships with non-fractal morphometric parameters. This suggests that both fractal dimensions are influenced by several shared factors, though they characterize different aspects of the fractal configuration.

In our previous study, the Minkowski dimension of the cerebellar white matter was found to have a strong negative correlation with age [37]. It was hypothesized that the Minkowski dimension (and its decrease with age) was most influenced by the thickness of the white matter branches and the age-related decrease in branch thickness. Conversely, the Hausdorff dimension determined in this study did not show statistically significant correlations with age. This dimension is determined solely by the degree of branching of the white matter, without considering age-related changes and branch thickness. Therefore, this type of fractal dimension may be particularly informative for biological and anthropological studies, the study of cerebellar development in its phylogenesis and ontogenesis, as well as for identifying developmental disorders – such as diagnosing malformations and differentiating malformations from atrophic changes in the cerebellum (where a decrease in Minkowski dimension might be expected with atrophy, while the Hausdorff dimension would remain unchanged; conversely, cerebellar maldevelopment would likely show a decrease specifically in the Hausdorff dimension).

The fractal dimensions showed significant correlations with the absolute sizes of the cerebellar vermis (cross-sectional perimeter and area). Therefore, it can be inferred that the increase in the absolute size of the cerebellum (in both phylogenesis and ontogenesis) leads to a more complex spatial configuration, manifested by an increase in the

Table 5
Statistical parameters of the ratios of the number of white matter branches in the cerebellum belonging to different iterations (n = 100).

Ratio of number of branches	Sex group	M	m	σ	CV, %	min	Q1	Me	Q3	max
2nd to 1st iteration	Entire sample	1.88	0.02	0.24	12.82	1.25	1.71	1.88	2.00	2.57
	Males	1.94	0.03	0.20	10.25	1.63	1.75	2.00	2.00	2.43
	Females	1.82	0.04	0.27	14.63	1.25	1.63	1.86	2.00	2.57
3rd to 2nd iteration	Entire sample	1.76	0.02	0.20	11.53	1.35	1.64	1.76	1.86	2.40
	Males	1.74	0.03	0.19	11.04	1.35	1.60	1.74	1.86	2.17
	Females	1.79	0.03	0.21	11.91	1.35	1.65	1.79	1.92	2.40
4th to 3rd iteration	Entire sample	1.82	0.02	0.20	11.29	1.36	1.68	1.80	1.95	2.48
	Males	1.84	0.03	0.22	11.81	1.36	1.69	1.82	1.99	2.48
	Females	1.79	0.03	0.19	10.68	1.39	1.67	1.78	1.92	2.30

Table 6
Descriptive statistics for fractal dimension values of cerebellar white matter determined by "box counting" method (n = 30).

Sex group	M	SEM	SD	CV, %	min	Q1	Me	Q3	max
Entire sample	1.486	0.013	0.070	4.715	1.345	1.434	1.487	1.542	1.629

Table 7
Descriptive statistics for fractal dimension values of cerebellar white matter determined by novel "contour scaling" method (n = 100).

Sex group	M	SEM	SD	CV, %	min	Q1	Me	Q3	max
Entire sample	1.697	0.010	0.099	5.838	1.478	1.630	1.702	1.775	1.913
Males	1.721	0.013	0.094	5.459	1.478	1.668	1.730	1.784	1.890
Females	1.674	0.014	0.099	5.940	1.502	1.600	1.651	1.748	1.913

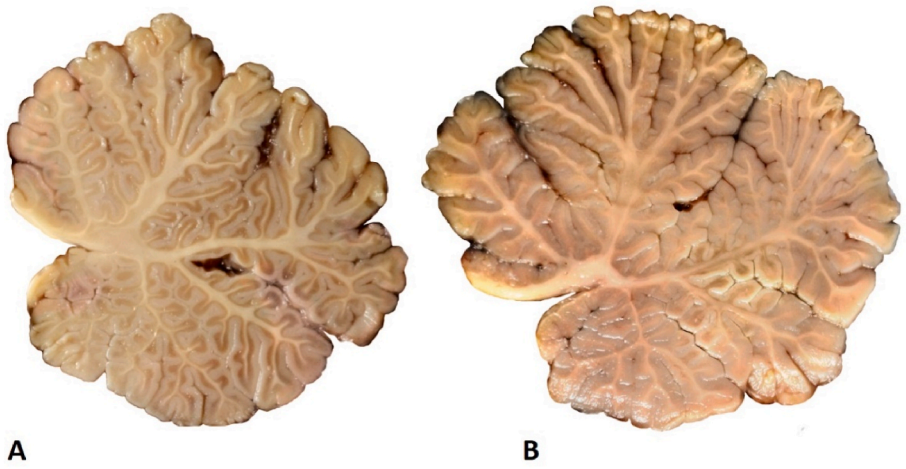

Fig. 17. Cerebellum with relatively low (A, fractal dimension = 1.579) and relatively high (B, fractal dimension = 1.851) values of fractal dimension determined by novel "contour scaling" method.

Table 8
Descriptive statistics for non-fractal morphometric parameters of the cerebellum (n = 100).

Parameter	Sex group	M	SEM	SD	CV, %	min	Q1	Me	Q3	max
Weight of the cerebellum, g	Entire sample	143.51	1.69	16.80	11.71	103	130	146	153.5	181
	Males	151.84	2.03	14.22	9.36	119	144	152	162	181
	Females	135.34	2.14	15.13	11.18	103	123.25	137	147	165
Cross-sectional area of the vermis, cm^2	Entire sample	10.50	0.12	1.16	11.05	7.66	9.68	10.39	11.14	13.44
	Males	10.92	0.17	1.19	10.89	8.92	10.07	10.77	11.85	13.44
	Females	10.08	0.14	0.97	9.67	7.66	9.40	10.13	10.61	12.73
Perimeter of the vermis cross section, cm	Entire sample	14.00	0.08	0.84	6.03	11.94	13.41	14.05	14.54	15.67
	Males	14.21	0.12	0.82	5.77	12.46	13.66	14.22	14.72	15.54
	Females	13.80	0.12	0.83	6.00	11.94	13.19	13.80	14.37	15.67
Perimeter-to-area ratio	Entire sample	1.34	0.01	0.09	6.36	1.14	1.29	1.35	1.40	1.56
	Males	1.31	0.01	0.09	6.66	1.14	1.23	1.32	1.37	1.48
	Females	1.37	0.01	0.07	5.11	1.23	1.34	1.38	1.41	1.56
Shape factor (circularity)	Entire sample	0.67	0.004	0.04	6.07	0.58	0.64	0.67	0.70	0.84
	Males	0.68	0.01	0.04	6.57	0.60	0.64	0.68	0.71	0.84
	Females	0.67	0.01	0.04	5.35	0.58	0.64	0.67	0.69	0.75

Table 9
Correlations between fractal dimension and non-fractal morphometric parameters of the cerebellum.

Parameter	Fractal dimension ("contour scaling" method)	Fractal dimension ("box counting" method)	Weight of the cerebellum	Cross-sectional area of the vermis	Perimeter of the vermis cross section	Perimeter-to-area ratio	Shape factor (circularity)
Fractal dimension ("contour scaling" method)	–	0.495*	0.299*	0.434*	0.521*	−0.268*	−0.241*
Fractal dimension ("box counting" method)	0.495*	–	0.485*	0.413*	0.434*	−0.387*	0.042
Weight of the cerebellum	0.299*	0.485*	–	0.539*	0.529*	−0.437*	−0.063
Cross-sectional area of the vermis	0.434*	0.413*	0.539*	–	0.863*	−0.888*	0.085
Perimeter of the vermis cross section	0.521*	0.434*	0.529*	0.863*	–	−0.545*	−0.426*
Perimeter-to-area ratio	−0.268*	−0.387*	−0.437*	−0.888*	−0.545*	–	−0.521*
Shape factor (circularity)	−0.241*	0.042	−0.063	0.085	−0.426*	−0.521*	–

*– $p < 0.05$.

Table 10
Correlations between fractal dimension, non-fractal morphometric parameters of the cerebellum and age.

Parameter	Entire sample	Males	Females
Fractal dimension ("contour scaling" method)	−0.182	−0.115	−0.087
Weight of the cerebellum	−0.479*	−0.356*	−0.370*
Cross-sectional area of the vermis	−0.352*	−0.250	−0.245
Perimeter of the vermis cross section	−0.349*	−0.251	−0.324*
Perimeter-to-area ratio	0.259*	0.170	0.079
Shape factor (circularity)	0.065	0.049	0.278*

*– $p < 0.05$.

branching degree of the white matter. As the cross-sectional area increases, the structural elements of the cerebellum (its folia, white matter branches) do not "scale up"; instead, their number increases.

This pattern accounts for the differences in fractal dimensions between males and females: males have statistically larger absolute cerebellar sizes, which leads to a higher degree of white matter branching compared to females. An interesting feature is that females more often exhibit a greater number of primary branches, but these branches further branch less compared to males. In previous studies that included fractal analysis of cerebellar white matter, no differences in fractal dimensions between males and females were identified [32,33]. This difference can be explained as follows. The aforementioned studies used modifications of the "box counting" method, which determines the Minkowski dimension, while the present study calculated the Hausdorff dimension. The Hausdorff dimension primarily depends on the number of branches across different iterations and is not influenced by branch thickness. Although the Minkowski dimension is also affected by the degree of white matter branching, this is not the sole factor influencing this fractal dimension. Branch thickness and the uniformity of space filling by the white matter are also important factors. Therefore, even with different degrees of white matter branching (i.e., different numbers of branches and Hausdorff dimension values), the white matter in male and female cerebella may exhibit similar levels of space filling. The male cerebellum has a larger cross-sectional area, which suggests an increase in the number of white matter branches and a higher Hausdorff dimension. However, as the number of branches increases and fills the available space (which also increases), the Minkowski dimension may remain unchanged.

The developed method of fractal analysis can be adapted for the study of other similar dendritic fractal structures, such as vascular networks, bronchial trees, ductal systems of glands, dendritic trees of neurons, and other quasi-fractal structures in the human and animal bodies that have a tree-like fractal pattern of development. In our view, the most suitable objects for the "contour scaling" method are canopy-like (umbrella-like) fractal trees (including natural fractals that resemble them), which have terminal iteration branches that reach a surface (or form a boundary). This feature enables the creation of contours that follow the terminations of these branches and allows for effective contour scaling.

To adapt the developed "contour scaling" method for studying other fractal structures, it is first necessary to determine how to define the contour that outlines the structure. This contour may pass through the terminals of the branches from the final iteration (touching them), follow the surface of the studied structure, or correspond to the boundaries of a specific area within which the fractal tree branches (area of blood supply, lobule of the gland, leaf of plant, etc.). Next, it is important to establish a control point to organize the series of scaled contours. This point can be the branching origin of a given structure. The following step involves determining the number of iterations of the fractal tree. This can be done by scaling the contour in small increments (5 %, as in the present study, or another interval may be used). By plotting the natural logarithm of the number of intersected branches (ln (N)) against the natural logarithm of the contour scaling factor (ln (Msc)), the number of "steps" on the resulting graph can be identified, corresponding to the branches of different iterations. This allows the determination of the number of iterations and the contour scales that best match the branches of a specific iteration. Afterward, the number of stages of fractal analysis corresponding to the defined iterations of the fractal tree's branching should be used.

In the case of studying multifractals, such a graph may appear irregular. Therefore, the intervals between iterations may differ from those in monofractals. To develop a methodology for studying multifractals, two approaches can be used: one can determine the number of iterations and the corresponding scales (which are likely to have irregular intervals) and conduct the analysis as for monofractals, calculating a single fractal dimension value, or identify several ranges with monofractal behavior and calculate the fractal dimension for each range separately, as in the study of monofractals. In the case of studying vascular networks, it is possible to conduct a fractal analysis of individual branches of the vessel and determine the fractal dimension for each one separately.

The developed fractal analysis method may have some important clinical implications. The novel "contour scaling" method could be applied in clinical practice for diagnostic purposes, specifically for diagnosing cerebellar malformations and differentiating them from acquired atrophic changes in the cerebellum. Combining the "contour scaling" method with the "box counting" method will enhance

diagnostic accuracy and identify anomalies in cerebellar anatomy that are difficult to quantify using conventional morphometric methods derived from Euclidean geometry. The ability to adapt the developed method for studying other fractal trees will enable its application in research involving angiograms, contrast X-rays of gland ducts, bronchial trees, and other similar structures.

5.1. Limitations of the study

The main limitations of using the developed "contour scaling" method are as follows. First, the type of structure being studied is crucial – this fractal analysis method can only be used for structures with a tree-like pattern of organization. The tree-like structures examined must have clearly defined terminal branches or regional boundaries that allow for the creation of a contour for scaling. If the tree-like structure has an overly irregular configuration, it may complicate the fractal analysis, particularly in determining the number of iterations (in fractal trees closer to artificial fractals, the number of iterations is more likely to be easily determined, while irregular branching complicates this analysis) and the corresponding contour scales for further fractal analysis. Since branch identification is done manually, there is a potential for errors in counting. Therefore, further development of image analysis software with automated counting capabilities will help improve the accuracy of the obtained results. In the context of conducting fractal analysis of the cerebellum, a limitation may be insufficient image quality (e.g., magnetic resonance brain images obtained with a low magnetic field scanner), which may complicate clear identification of intersected branches.

6. Conclusion

The Arbor vitae cerebelli can be considered a natural fractal tree. Based on the fractal approach to the anatomy of the cerebellar white matter, a novel "contour scaling" method of fractal analysis was developed. This method is adapted to the anatomical features of the cerebellum and allows for the determination of its fractal (Hausdorff) dimension. The Hausdorff dimension of the cerebellar Arbor vitae, as determined by this method, does not change with age but increases with the absolute size of the cerebellum, indicating an increase in its structural complexity. The novel "contour scaling" method of fractal analysis can be adapted for the quantitative assessment of other anatomical structures that have a tree-like branching pattern of organization.

Ethical statement

The study was conducted in accordance with the World Medical Association Declaration of Helsinki: Ethical principles for medical research involving human subjects. The collection and investigation of cadaveric specimens were conducted in accordance with current Ukrainian legislation. This study does not use unethically sourced organs or tissue, including from executed prisoners or prisoners of conscience, consistent with recommendations by Global Rights Compliance on Mitigating Human Rights Risks in Transplantation Medicine. The study was approved by the Commission on Ethics and Bioethics of Kharkiv National Medical University (minutes of the meeting No. 5, February 1, 2023) for studies involving humans.

Funding

This research did not receive any specific grant from funding agencies in the public, commercial, or not-for-profit sectors.

CRediT authorship contribution statement

Nataliia Maryenko: Writing – original draft, Visualization, Methodology, Investigation, Formal analysis, Data curation, Conceptualization. **Oleksandr Stepanenko:** Writing – review & editing, Validation, Supervision, Project administration, Methodology, Conceptualization.

Declaration of competing interest

The authors declare that they have no known competing financial interests or personal relationships that could have appeared to influence the work reported in this paper.

Acknowledgments

The authors sincerely thank those who donated their bodies to science so that anatomical research could be performed. Results from such research can potentially increase mankind's overall knowledge that can then improve patient care. Therefore, these donors and their families deserve our highest gratitude.

Appendix A. Supplementary data

Supplementary data to this article can be found online at https://doi.org/10.1016/j.tria.2024.100352.

References

[1] W.I. Welker, The significance of foliation and fissuration of cerebellar cortex. The cerebellar folium as a fundamental unit of sensorimotor integration, Arch. Ital. Biol. 128 (2–4) (1990) 87–109.
[2] O. Larsell, J. Jansen, The Comparative Anatomy and Histology of the Cerebellum, University of Minnesota Press, Minneapolis, 1972.
[3] K. Heuer, N. Traut, A.A. de Sousa, S.L. Valk, J. Clavel, R. Toro, Diversity and evolution of cerebellar folding in mammals, Elife 12 (2023) e85907, https://doi.org/10.7554/eLife.85907.
[4] A. Sudarov, A.L. Joyner, Cerebellum morphogenesis: the foliation pattern is orchestrated by multi-cellular anchoring centers, Neural Dev. 2 (2007) 26, https://doi.org/10.1186/1749-8104-2-26.
[5] R.V. Sillitoe, A.L. Joyner, Morphology, molecular codes, and circuitry produce the three-dimensional complexity of the cerebellum, Annu. Rev. Cell Dev. Biol. 23 (2007) 549–577, https://doi.org/10.1146/annurev.cellbio.23.090506.123237.
[6] P. Demaerel, Abnormalities of cerebellar foliation and fissuration: classification, neurogenetics and clinicoradiological correlations, Neuroradiology 44 (8) (2002) 639–646, https://doi.org/10.1007/s00234-002-0783-1.
[7] S. Patel, A.J. Barkovich, Analysis and classification of cerebellar malformations, AJNR Am J Neuroradiol 23 (7) (2002) 1074–1087.
[8] M. Sasaki, H. Oikawa, S. Ehara, Y. Tamakawa, S. Takahashi, H. Tohgi, Disorganised unilateral cerebellar folia: a mild form of cerebellar cortical dysplasia? Neuroradiology 43 (2) (2001) 151–155, https://doi.org/10.1007/s002340000340.
[9] D. Shyian, D. Galata, S. Potapov, V. Gargin, Peculiarities of the cerebellum nuclei in aged persons, Georgian Med. News 253 (2016) 110–115.
[10] K. Hayakawa, Y. Konishi, T. Matsuda, et al., Development and aging of brain midline structures: assessment with MR imaging, Radiology 172 (1) (1989) 171–177, https://doi.org/10.1148/radiology.172.1.2740500.
[11] T. Supprian, G. Ulmar, M. Bauer, et al., Cerebellar vermis area in schizophrenic patients - a post-mortem study, Schizophr. Res. 42 (1) (2000) 19–28, https://doi.org/10.1016/s0920-9964(99)00103-6.
[12] S. Han, Y. An, A. Carass, J.L. Prince, S.M. Resnick, Longitudinal analysis of regional cerebellum volumes during normal aging, Neuroimage 220 (2020) 117062, https://doi.org/10.1016/j.neuroimage.2020.117062.
[13] J. Stalter, V. Yogeswaran, W. Vogel, P. Sörös, C. Mathys, K. Witt, The impact of aging on morphometric changes in the cerebellum: a voxel-based morphometry study, Front. Aging Neurosci. 15 (2023) 1078448, https://doi.org/10.3389/fnagi.2023.1078448.
[14] K.E. Yopak, T.J. Lisney, S.P. Collin, J.C. Montgomery, Variation in brain organization and cerebellar foliation in chondrichthyans: sharks and holocephalans, Brain Behav. Evol. 69 (4) (2007) 280–300, https://doi.org/10.1159/000100037.
[15] T.J. Lisney, K.E. Yopak, J.C. Montgomery, S.P. Collin, Variation in brain organization and cerebellar foliation in chondrichthyans: batoids, Brain Behav. Evol. 72 (4) (2008) 262–282, https://doi.org/10.1159/000171489.
[16] A.N. Iwaniuk, P.L. Hurd, D.R. Wylie, Comparative morphology of the avian cerebellum: I. Degree of foliation, Brain Behav. Evol. 68 (1) (2006) 45–62, https://doi.org/10.1159/000093530.
[17] F. Cunha, C. Gutiérrez-Ibáñez, K. Racicot, D.R. Wylie, A.N. Iwaniuk, A quantitative analysis of cerebellar anatomy in birds, Brain Struct. Funct. 226 (8) (2021) 2561–2583, https://doi.org/10.1007/s00429-021-02352-2.
[18] R.F.M. Bispo, A.J.C. Ramalho, L.C.B. Gusmão, A.P.H. Cavalcante, A.C. Rocha, C. F. Sousa-Rodrigues, Cerebellar vermis: topography and variations, Int. J. Morphol. 28 (2) (2010) 439–443, https://doi.org/10.4067/S0717-95022010000200018.

[19] B.B. Mandelbrot, The Fractal Geometry of Nature, W.H. Freeman and Company, San Francisco, 1982.
[20] J. Feder, Fractals, Plenum Press, New York, 1988, p. 284.
[21] H. Fractals Lauwerier, Endlessly Repeated Geometric Figures, Princeton University Press, Princeton, NJ, 1991, pp. 67–77.
[22] M. Fernández-Martínez, M.A. Sánchez-Granero, How to calculate the Hausdorff dimension using fractal structures, Appl. Math. Comput. 264 (2015) 116–131, https://doi.org/10.1016/j.amc.2015.04.059.
[23] F. Beck, M. Burch, T. Munz, L. Di Silvestro, D. Weiskopf, Generalized Pythagoras trees: a fractal approach to hierarchy visualization, in: S. Battiato, S. Coquillart, J. Pettré, R. Laramee, A. Kerren, J. Braz (Eds.), Computer Vision, Imaging and Computer Graphics - Theory and Applications. VISIGRAPP 2014. Communications in Computer and Information Science 550 (2015) 49–64, https://doi.org/10.1007/978-3-319-25117-2_8. Cham: Springer.
[24] C. Browne, Efficient Pythagorean trees: greed is good 31 (4) (2007) 610–616, https://doi.org/10.1016/j.cag.2007.04.003.
[25] A.Y. Stepanenko, Structural organization and variant anatomy of the human cerebellar vermis white matter, Medicine today and tomorrow 3 (52) (2011) 5–10. Available from: https://repo.knmu.edu.ua/handle/123456789/1952.
[26] E.E. Underwood, Quantitative Stereology, Addison-Wesley, London, 1970.
[27] A.L. Karperien, H.F. Jelinek, Box-counting fractal analysis: a primer for the clinician, Adv Neurobiol 36 (2024) 15–55, https://doi.org/10.1007/978-3-031-47606-8_2.
[28] A.L. Karperien, H.F. Jelinek, ImageJ in computational fractal-based neuroscience: pattern extraction and translational research, Adv Neurobiol 36 (2024) 795–814, https://doi.org/10.1007/978-3-031-47606-8_40.
[29] H.F. Jelinek, E. Fernandez, Neurons and fractals: how reliable and useful are calculations of fractal dimensions? J. Neurosci. Methods 81 (1–2) (1998) 9–18, https://doi.org/10.1016/s0165-0270(98)00021-1.
[30] D. Cornforth, H.F. Jelinek, Monofractal and multifractal analysis for interpretation of function-structure relationships in finite size biological material, in: Classification and Application of Fractals: New Research, 2012, pp. 303–324.
[31] D.A. Sholl, Dendritic organization in the neurons of the visual and motor cortices of the cat, J. Anat. 87 (4) (1953) 387–406.
[32] J.Z. Liu, L.D. Zhang, G.H. Yue, Fractal dimension in human cerebellum measured by magnetic resonance imaging, Biophys. J. 85 (6) (2003) 4041–4046, https://doi.org/10.1016/S0006-3495(03)74817-6.
[33] Y.T. Wu, K.K. Shyu, C.W. Jao, et al., Fractal dimension analysis for quantifying cerebellar morphological change of multiple system atrophy of the cerebellar type (MSA-C), Neuroimage 49 (1) (2010) 539–551, https://doi.org/10.1016/j.neuroimage.2009.07.042.
[34] E. Akar, S. Kara, H. Akdemir, A. Kırış, Fractal dimension analysis of cerebellum in Chiari Malformation type I, Comput. Biol. Med. 64 (2015) 179–186, https://doi.org/10.1016/j.compbiomed.2015.06.024.
[35] C. Marzi, S. Ciulli, M. Giannelli, et al., Structural complexity of the cerebellum and cerebral cortex is reduced in spinocerebellar ataxia type 2, J. Neuroimaging 28 (6) (2018) 688–693, https://doi.org/10.1111/jon.12534.
[36] G. Zhao, K. Walsh, J. Long, W. Gui, K. Denisova, Reduced structural complexity of the right cerebellar cortex in male children with autism spectrum disorder, PLoS One 13 (7) (2018) e0196964, https://doi.org/10.1371/journal.pone.0196964.
[37] A.Y. Stepanenko, N.I. Maryenko, Fractal analysis of the human cerebellum white matter, World of medicine and biology 3 (61) (2017) 145–149, https://doi.org/10.26724/2079-8334-2017-3-61-145-149.
[38] N.I. Maryenko, O.Y. Stepanenko, Fractal analysis of anatomical structures linear contours: modified Caliper method vs Box counting method, Rep. of Morph. 28 (1) (2022), https://doi.org/10.31393/morphology-journal-2022-28(1)-03, 17-6.